considered case, all three algorithms perform well. The goal for the norm of the objective function (which is comparable to the maximum reflection coefficient in the considered band) to fall below 0.003 is obtained after approximately 2 h of calculations. The program was run on a PC 486DX/66 MHz with 8 Mbytes of random access memory (RAM).

Presented here is another example to show the different performance of the investigated methods with different starting points. Optimization of a dielectric support in the 7-mm coaxial line is considered. The structure is presented in Fig. 3(a). In case of optimization with a bad (far from optimum) starting point, both gradient methods (DFP and CJG) fail [as seen in Fig. 3(b).] while the Powell method, after 10 min, produces a result sufficiently good to start the second (precise) stage of optimization. It should be noted that using the first stage results of the Powell method as the starting point of the second stage produces good convergence of any of the three methods. Comparison of the performance of the three above-mentioned methods in application to the considered problems can be summarized in the following way.

- The Powell method was found to be slightly less efficient than gradient methods but more reliable when starting from a distant point. It was also found more robust when strong constraints imposed on circuit dimensions are considered. It was found to be the most universal and practically useful of the three considered methods.
- Both considered gradient methods were found less useful. It is also worth noting that out of the two gradient methods considered, the DFP method performs slightly better.

## IV. More Examples of Application

An example of a transformer presented originally in [13] is considered here. This type of transformer provides very good performance and small size. However, at very high frequencies the fringing fields at the junctions of the consecutive sections may have a very important effect on the characteristics of the device. This effects would be very difficult to estimate and correct in the classical model. In the example presented in Fig. 4, a six-section nonsynchronous transformer is taken for a 5–13 GHz frequency band to match 20 $\Omega$ line (left) to 80 $\Omega$ line (right), composed of the sections of 80 and 20 $\Omega$ lines of lengths $l_0$–$l_1$. In this case, the noncompensated application of the design after [13] produces quite a poor result due to the presence of the fringing fields. This design has been used as the starting point of the authors' optimization. The final result presented as a continuous line in Fig. 4(b) is much better and very close to the expectations. Table I presents the lengths $l_0$–$l_1$ before and after optimization.

Another example is a commercial N to LCM connector. The authors have taken the original dimensions [Fig. 5(a)] and run the optimization, with 14 variables, assuming the usable frequency band up to 8 GHz. The calculation time was approximately 6.5 h on a Pentium 100 MHz. The resulting dimensions are shown in Fig. 5(b) and the improvement in the $|S_{11}|$ performance is shown in Fig. 5(c).

## V. Conclusion

In this paper, the approach to the improved design of passive coaxial devices based on EM analysis in an optimization loop proved both accurate and effective. In simple cases, it produces the results with industrially acceptable accuracy on a fast PC within 0.5–2 h. Even in the cases of complicated structures with up to 14 variables, good results were obtained within 5–10 h. The method has been applied in industrial design with very positive feedback from engineers.

## References


[1] W. Gwarek, "Computer-aided analysis of arbitrarily shaped coaxial discontinuities," *IEEE Trans. Microwave Theory Tech.*, vol. 36, pp. 337–342, Feb. 1988.

[2] ____, *Quick-Wave User's Manual.* Duisburg, Germany: ArguMens, 1990.

[3] P. P. M So, W. J. R.Hoefer, J. W. Bandler, R. M. Biernacki, and S. H. Chen, "Hybrid frequency/time domain field theory based CAD of microwave circuits," in *23rd European Microwave Conf. Dig.*, Madrid, Spain, Sept. 1993, pp. 218–219.

[4] P. P. M So and W. J. R. Hoefer, "FD-TLM techniques for field-based optimization of electromagnetic structures," in *1994 IEEE MTT-S Dig.*, San Diego, CA, pp. 423–426.

[5] J. W. Bandler, R. M. Biernacki, and S. H. Chen, "Optimization technology for microwave circuit modeling and design," in *25th European Microwave Conf.*, Bologna, Italy, Sept. 1995, pp. 101–108.

[6] ____, "Fully automated space mapping optimization of 3-D structures," in *1996 IEEE MTT-S Dig.*, San Francisco, CA, pp. 753–756.

[7] ____, "Parametrization of arbitrary geometrical structures for automated electromagnetic optimization," in *1996 IEEE MTT-S Dig.*, San Francisco, CA, pp. 1059–1062.

[8] R. C. Tupynamba and A. S. Omar, "The synthesis of passive circuits using the FDTD," in *1996 IEEE MTT-S Dig.*, San Francisco, CA, pp. 749–752.

[9] J. W. Bandler and S. H. Chen, "Circuit optimization: The state of the art," *IEEE Trans. Microwave Theory Tech.*, vol. 36, pp. 424–443, Feb. 1988.

[10] E. Polak, *Computational Methods of Optimization—A Unified Approach.* New York: Academic, 1970.

[11] G. Matthaei, L. Young, and E. M. T. Jones, *Microwave Filters, Impedance Matching Networks and Coupling Structures.* Norwood, MA: Artech House, 1980, pp. 365–372.

[12] W. K. Gwarek, "Analysis of an arbitrarily shaped planar circuit—A time domain approach," *IEEE Trans. Microwave Theory Tech.*, vol. MTT-33, pp. 1067–1072, Oct. 1985.

[13] S. Rosloniec, "Algorithms for the computer-aided design of nonsynchronous, noncommensurate transmission-line impedance transformers," *Int. J. Microwave Millimeter-Wave Comp.-Aided Eng.*, vol. 4, no. 3, pp. 307–314, Mar. 1994.


# Automated Optimization of a Waveguide-Microstrip Transition Using an EM Optimization Driver

Min Zhang and Thomas Weiland

***Abstract*—An electromagnetic (EM) optimization driver is introduced which makes optimization of electromagnetic components fully automatic. The driver is composed of an EM simulator and an optimizer. As a test example, an optimum design of a waveguide–microstrip transition using the driver is demonstrated. The numerical design is verified by the measurement.**

## I. Introduction

In recent years, the rapid development of numerical techniques brings a lot of practical software packages available either in the

Manuscript received November 4, 1996; revised January 2, 1997.

M. Zhang is with Deutsches Elektronen-Synchrotron, MPY, Hamburg 22603 Germany.

T. Weiland is with FB18, Technische Hochschule Darmstadt, Darmstadt 64289 Germany.

Publisher Item Identifier S 0018-9480(97)03098-6.

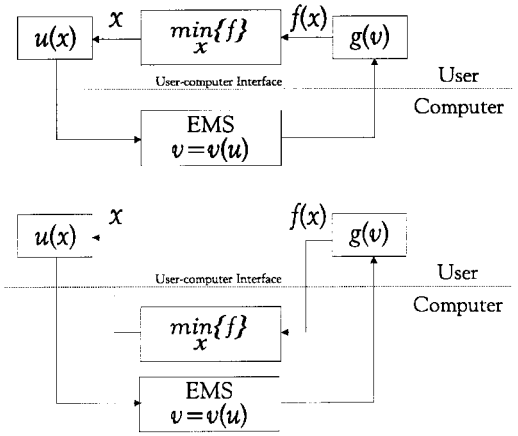


Fig. 1. Two optimization modes min $\{f\}$ represents the optimizer, $x$—the optimization vector, $u$—EMS input vector, EMS for EM simulator, $v$—EMS output vector, $g(x)$—the goal function.

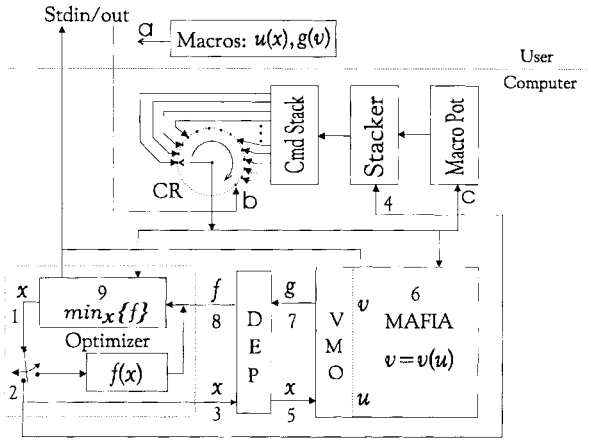


Fig. 2. Detailed Structure of MAFIA Optimization Driver. DEP is composed of a large common block area: VMO—variable mapping operator, does the mapping of $x$ to $u$ and $v$ to $g$, which are both defined by the user. The command reader (CR) always checks the command stack first, as "its handle is rotating clockwise." It ignores any inputs from Stdin unless the stack is read empty. $f(x)$ is the built-in test goal function generator. A complete cycle of the optimization loop is indicated by the numbers in sequence: 1. new search point $x$; 2. switch to EMS; 3. put $x$ to DEP; 4. invoke EMS; 5. read $x$ from DEP and convert to $u$; 6. do simulations; 7. output result $v$; 8. give control back to the optimizer; 9. do a new round of decision-making.

market or in various laboratories. Most of the electromagnetic (EM) software packages are, however, used to do field or circuit analyzes. There are only a few of them which are capable of handling synthesis problems. To make design procedures more versatile, combining EM simulators with optimizers would be the way to go. This combined environment is referred to as an EM optimizer or an EM optimization driver.

In this paper, one such EM optimizer is presented, which is realized with the general purpose EM software package—MAFIA [1]. The driver is composed of the MAFIA EM simulator and an optimizer containing various optimization methods like DFP, BFGS [2], gradient associated conjugate direction (GaCD) [3], constrained optimization using partials (COUP), evolution strategy (ES) [4], etc.

There are now increasing numbers of papers on EM optimizers [5], [6]. Most of them are for substrate-based circuit design using special techniques, which are usually more central processing unit (CPU)-effective. Many new optimization methods are developed which are suitable for numerical optimizations, e.g. COUP, ES, and space mapping (SM) [5]. As far as is known, the MAFIA EM optimizer presented in this paper is the first of its kind which is oriented to dealing with a broad spectrum of EM optimization problems with its built-in global/local constrained/nonconstrained optimization methods. The authors successfully apply it to many practical designs, e.g., particle accelerating cavity, low crosspolarization antenna, traction magnet, microstrip transition, etc.

To demonstrate the effectiveness of the driver, the authors take an $X$-band waveguide-microstrip transition as an example. ES is used for global optimum searches and GaCD for local ones. The whole optimization process is fully automated.

## II. The Optimization Driver

The MAFIA optimization driver supports two optimization modes (see Fig. 1). For mode A, optimization strategies are coded in the MAFIA command language, while for mode B they are built-in. Here, the authors only discuss the realization of mode B. The overall structure of the driver is shown in Fig. 2. It can be seen that with data exchange plot (DEP), the interface becomes very simple and easy to debug. It requires a minimum change to both the optimizer and the simulator. Both blocks are well isolated from interference from either side when run in their stand-alone mode.

## III. Transition Optimum Design

### A. The Transition Setup

The transition was first proposed by J. H. C. van Heuven in 1976 [7]. He got his transition geometry by experiments. The authors propose to do the design by the optimization driver. It should be noted that this is not intended to be an exhausting design but rather a demonstration suitable for this issue.

The design bandwidth is 9.6–10.4 GHz. An initial geometry which delivers an average $S_{21}$ equal to 0.509 is chosen. The goal is to have $\overline{S_{21}}$ as close to 1 as possible. This is mainly determined by two factors. One is the ems' field simulation accuracy. The other is the stop criteria set for the optimizer. In this case, since the MAFIA ems is a finite difference code, the former is more dominant, unless the mesh is very fine.

For demonstration, a relatively coarse mesh is used: $n_x \times n_y \times n_z = 12 \times 11 \times 59 = 7788$ mesh points. To avoid discretization noises, this mesh is fixed throughout the whole optimization process.

The transition setup is shown in Fig. 3. It is composed of two back-to-back transitions, which accommodates a precision $S_{21}$ measurement.

### B. Optimization Methods

Two methods are used: GaCD and ES. The former is for local extremum searches while the latter is for global optimum area detection.

GaCD is a conjugate direction method. It is found that GaCD is among the most effective conjugate-based methods like BFGS, DFP, etc. In many cases, it is even superior to those methods [3].

ES was first proposed by I. Rechenberg in the 1970's [8]. The ES used here uses a predefined variation step function. Three terms may be used to describe the ES: fruit, seed, and variation. Fruit and seed are optimization directions. A fruit determines a general search direction while a seed determines an omni-directional vector in a small region, whose size is statistically controlled by the variation step. For further information, refer to [4].

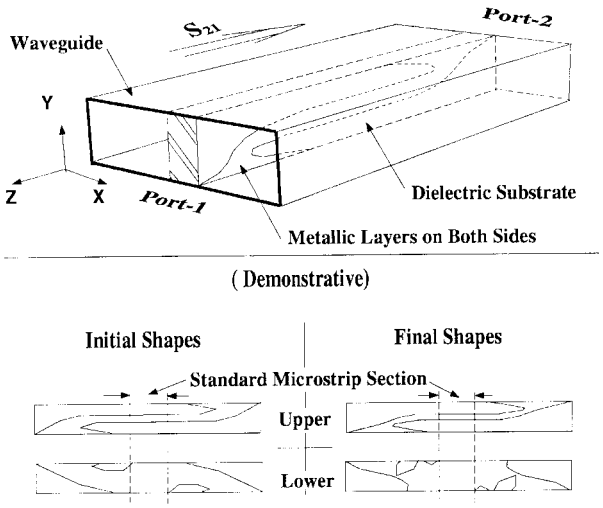


Fig. 3. Transition setup.

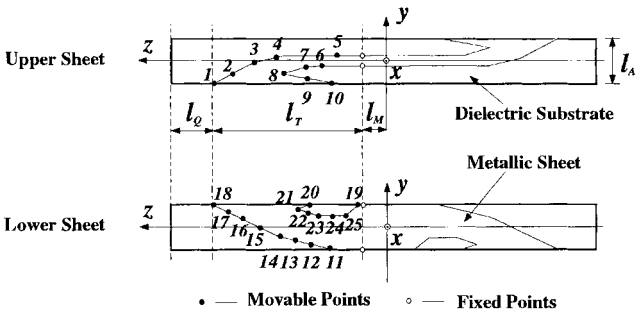


Fig. 4. Definition of optimization vector.

### C. Definition of the Optimization Problem

The authors take a total of 25 points along the profiles of the upper and the lower metallic sheets as optimization vector $\boldsymbol{X}$ (Fig. 4). Points #21 to #25 can be moved in both $y$- and $z$-directions while the rest only in the $z$-direction. It is, therefore, a problem of 30° of freedom. The definition range is $-l_A/2 \le y \le l_A/2$, $l_M \le z \le (l_M + l_T)$. The whole set of the definition ranges for $\boldsymbol{X}$ is denoted by $\mathcal{X} \subset \Re^{30}$. The goal function is defined as

$$\mathcal{G}(\boldsymbol{X}) \equiv \overline{S_{21}}(\boldsymbol{X})$$

with $\overline{S_{21}}$ being an average of $|S_{21}|$ from 9.6 to 10.4 GHz. The optimization problem can then be expressed as

$$\mathcal{G}^* \equiv \max\{\mathcal{G}(\boldsymbol{X})\} \qquad \forall \boldsymbol{X} \in \mathcal{X}.$$

### D. Simulation Preparations

The operating mode of the transition is $H_{10}$. $l_M$, $l_Q$, and $l_T$ are chosen to be 10, 20, and 30 mm, respectively. $l_M$ makes transmission in the middle half waveguide less than 52 dB. $l_Q$ attenuates the first higher order mode ($H_{20}$) by 52 dB and the second by 74 dB. The driving signal used is given below:

$$s(t) = \begin{cases} 0 & t < 0 \\ \exp\{-[c_1\pi(t - c_2)]^2\}\cos[2\pi f_0(t - c_2)], & t \ge 0. \end{cases}$$

$c_2$ is a delay while $c_1$ determines the signal's bandwidth. The authors choose $c_1 = 8.4\times10^8$ and $c_2 = 1.1$ ns. Total simulation time ($T_{\text{total}}$) is determined by $4(t_d^Q + t_d^T + t_d^M) + 2c_2$, where $td^Q$, $t_d^T$, and $t_d^M$ are the delay in section Q, T, and M, respectively. $T_{\text{total}}$ is chosen to be 50 ns.

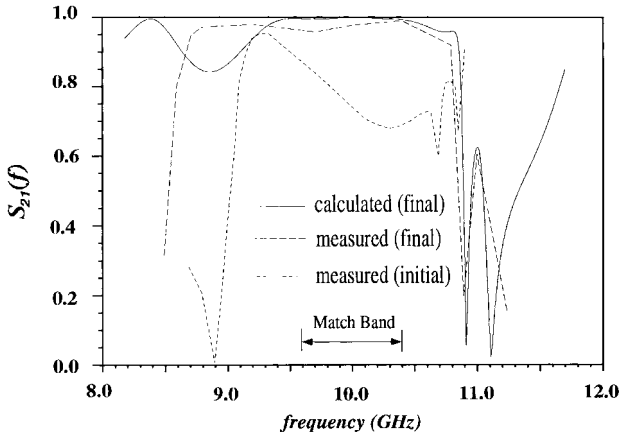


Fig. 5. Measured and calculated $S_{21}$ for final and initial structures.

TABLE I
STATISTIC DATA OF THE OPTIMIZATION

| | |
|---|---|
| $\overline{S_{21}}$ (initial) | 0.509 |
| $\overline{S_{21}}$ (final) | 0.996 |
| Relative Improvement of $\overline{S_{21}}$ | 95.5% |
| Total CPU (IBM-550) | 102.5 hours |
| Number of Field Simulations | 338 |
| CPU (per Field Simulation) | 0.29 hour |
| Number of optimization Loops | 7 |

### E. Simulation Results and Measurements

The initial and the final shapes are shown in Fig. 3. Table I lists some statistics of the optimization. The computing time is dependent on two main factors: ems speed and optimization methods' effectiveness.

The transitions are fabricated and measured. $\epsilon_r$ of the substrate is 2.2 and thickness $1.57 \pm 0.05$ mm. Fig. 5 shows the measured $S_{21}$ curves together with the calculated one. It is found that the measured $S_{21}$ is generally poorer than the calculated one. It is because ohmic losses and the mounting grooves of the structure were not taken into account in the simulation.

## IV. CONCLUSION

A realization of combining an optimizer with an existing EM simulator was presented. Simple concepts of data exchange pot and variable mapping operator were briefly introduced. They can be adopted for other existing simulation codes to make them optimization drivers. An example was given to show the usefulness of the driver. To have numerical optimization drivers practically acceptable, further work has to be done, especially on ems speed, optimization methods performance, and algorithm vectorization.

## REFERENCES

[1] T. Weiland *et al.* "Solution of Maxwell's equations," *Comput. Physics Commun.* vol. 72, pp. 22–39, 1992.
[2] D. A. Pierre, *Optimization Theory with Applications.* New York: Dover, 1986.
[3] M. Zhang, "The gradient associated conjugate direction method," *Appl. Computational Electromagnetics Soc. J.*, Nov. 1996.
[4] ——, "Numerical optimization of electromagnetic components," Ph.D. dissertation, Technische Hochschule Darmstadt, Germany, 1995.

[5] J. W. Bandler *et al.* "Electromagnetic optimization exploiting aggressive space mapping," *IEEE Trans. Microwave Theory Tech.*, vol. 43, pp. 2874–2882, Dec. 1995.
[6] J. W. Bandler *et al.* "Microstrip filter design using direct EM field simulation," *IEEE Trans. Microwave Theory Tech.*, vol. 42, pp. 1353–1359, July 1994.
[7] J. H. C. van Heuven, "A new integrated waveguide–microstrip transition," *IEEE Trans. Microwave Theory Tech.*, vol. MTT-24, pp. 144–147, Mar. 1976.
[8] I. Rechenberg, *Evolutionsstrategie, Optimierung Technischer Systeme Nach Prinzipien der Biologischen Evolution.* Stuttgart-Bad Cannstadt, Germany: Frommann-Holzboog, 1973.

# Spiral Super-Quadric Generatrix and Bodies of Two Generatrices in Automated Parameterization of 3-D Geometries

Branko M. Kolundzija and Antonije R. Djordjević

***Abstract*—Most of the methods that solve the surface integral equation (SIE) by the method of moments (MoM) use triangles and flat quadrilaterals for geometrical modeling. Many complex structures can be easily modeled by quadrilaterals combining spiral super-quadric generatrices and the concept of the body of two generatrices (BoTG). A BoTG is any body that can be obtained from two generatrices by applying a certain rule. Four simple rules for obtaining BoTG's are: 1) generalized rotation; 2) translation; 3) constant cut; and 4) connected generatrices. Spiral super-quadric generatrices enable efficient modeling of circles, arcs, ellipses, squares, rectangles, spirals, etc. Thus, a simple but fairly general algorithm for geometrical modeling is obtained, convenient for implementation in electromagnetic-field solvers.**

## I. Introduction

Starting from the equivalence theorem, any composite metallic and dielectric structure can be analyzed by using an surface integral equation (SIE). Such integral equations are usually solved by the method of moments (MoM). Most of the existing MoM methods use triangles [1], and flat quadrilaterals [2] for geometrical modeling. Any of these patches is completely defined by three or four nodes in space. In the case of user-friendly algorithms (e.g., WIPL [2]), nodes are defined by their $x$-, $y$-, and $z$-coordinates, and patches are defined by indices of the corresponding nodes. However, for relatively complex structures, such a way of defining a geometry can be very time-consuming. This difficulty can be overcome by introducing an automated parameterization of three-dimensional (3-D) geometries.

Most commercial electromagnetic-field solvers [3]–[5] model two-dimensional (2-D) and 3-D geometries in a similar way as AutoCAD [6], or can import structures from it. Many bodies of interest for electromagnetic modeling are represented by these solvers as bodies of revolution (BoR's) and bodies of translation (BoT's). BoR's and BoT's are usually obtained by revolution and translation of 2-D objects. In addition, there are particular options for creation of 2-D objects in the form of circles, arcs, ellipses, rectangles, etc. For example, a circular waveguide, simple and stepped coaxial lines can be modeled as BoR's, and a rectangular waveguide can be modeled as a BoT. However, these primitives cannot be used for modeling slightly complicated structures (e.g., a coaxial-line T-junction, transition from rectangular to circular waveguide, finite-thickness spiral inductor, etc.). Even AutoCAD with its sophisticated tools cannot model these structures in a simple way. Finally, note that it is very difficult to implement these sophisticated tools in new electromagnetic-field solvers.

The purpose of this paper is to show that all structures mentioned above, and many others, can be efficiently modeled by combining a spiral super-quadric generatrix and the concept of body of two generatrices (BoTG).

Manuscript received October 28, 1996; revised January 2, 1997.

The authors are with the Department of Electrical Engineering, University of Belgrade, Belgrade 11001, Yugoslavia.

Publisher Item Identifier S 0018-9480(97)03109-8.

## II. Spiral Super-Quadric Generatrix

Very often, the generatrix has the form of a circle, ellipse, square, rectangle, or rhomboid. Any of these primitives can be described by the super-quadric function. This function can be represented in the local $ps$-coordinate system as

$$\left(\frac{p}{a}\right)^{2/t}+\left(\frac{s}{b}\right)^{2/t}=1, \qquad a,\, b>0, \qquad t\geq 0. \tag{1}$$

$2a$ and $2b$ represent lengths of the main axes along $p$- and $s$-coordinates, and the parameter $t$ determines the general shape of this function. For example, an ellipse is obtained for $t=1$, a rectangle is obtained for $t=0$, and a rhomboid is obtained for $t=2$.

In order that arcs and spirals can also be defined, (1) is modified into the spiral super-quadric function, described by the following parametric equations:

$$p=qa(1+c\varphi)\cos\varphi, \qquad s=qb(1+c\varphi)\sin\varphi$$
$$(\cos\varphi)^{2/t}+(\sin\varphi)^{2/t}=q^{-2/t}, \qquad \varphi_1\leq\varphi\leq\varphi_2. \tag{2}$$

The parameter $\varphi$ is an angle measured from the $p$-coordinate axis, and takes values from $\varphi_1$ to $\varphi_2$. If $\varphi_2-\varphi_1<360^\circ$, various types of arcs are obtained. If $c$ is different from zero and $\varphi_2-\varphi_1>360^\circ$, various types of spiral functions are obtained.

In order that a generatrix can be used for creation of bodies consisting of quadrilaterals, it should be defined by a set of nodes in the $ps$-plane. In this paper, positions of these nodes are defined by angles $\varphi$:

$$\varphi_i=\varphi_1+(i-1)\frac{\varphi_2-\varphi_1}{n}, \qquad i=1,\cdots,n \tag{3}$$

where $n$ is the number of nodes.

In order that the executable code be user friendly, the following default values for the above parameters are recommended: $b/a=1$, $t=1$, $c=0$, $\varphi_1=0^\circ$, and $\varphi_2=360^\circ$. In that case, different shapes can be easily defined, as shown in Fig. 1(a): circle $(n=16,\, a=1)$, (b) ellipse $(n=16,\, a=1,\, b/a=0.5)$, (c) rectangle $(n=16,\, a=1,\, b/a=0.5,\, t=0)$, (d) rhomboid $(n=16,\, a=1,\, b/a=0.5,\, t=2)$, (e) spiral with circular turns $(n=32,\, a=0.4,\, c=1,\, \varphi_2=720^\circ)$, and (f) spiral with square-shaped turns $(n=32,\, a=0.4,\, c=1,\, \varphi_2=720^\circ,\, t=0)$.

## III. Bodies of Two Generatrices

Most of the bodies encountered in the design of microwave circuits can be modeled as a combination of BoTG's. A BoTG is any body that can be obtained by using two generatrices according to